International Journal of Solids and Structures 121 (2017) 75–85

Contents lists available at ScienceDirect

International Journal of Solids and Structures

journal homepage: www.elsevier.com/locate/ijsolstr

Strong sampling surfaces formulation for layered shells

G.M. Kulikov*, S.V. Plotnikova

Laboratory of Intelligent Materials and Structures, Tambov State Technical University, Sovetskaya, 106, Tambov 392000, Russia

ARTICLE INFO

Article history:
Received 23 February 2017
Revised 6 May 2017
Available online 15 May 2017

Keywords:
Elasticity
3D stress analysis
Layered shell
Sampling surfaces method

ABSTRACT

The strong SaS formulation for the three-dimensional (3D) stress analysis of layered shells is based on a new concept of SaS located at Chebyshev polynomial nodes throughout the layers and integration of the equilibrium equations of elasticity. The idea of the SaS method consists in choosing the arbitrary number of SaS parallel to the middle surface in order to introduce the displacements of these surfaces as basic shell unknowns. Such choice of unknowns with the use of the Lagrange polynomials in assumed approximations of displacements and strains through the layer thicknesses leads to a compact form of the layered shell formulation. The feature of the proposed approach is that all SaS are located inside the layers at Chebyshev polynomial nodes. The use of interfaces is avoided that makes possible to minimize uniformly the error due to the Lagrange interpolation. Therefore, the strong SaS formulation can be applied efficiently to the 3D analysis of layered composite shells.

1. Introduction

Three-dimensional (3D) analysis of layered composite plates and shells has received considerable attention during past thirty years (see survey articles of Wu et al., 2008 and Wu and Liu, 2016). There are at least five approaches to 3D exact solutions for layered plates and shells, namely, the Pagano approach (Pagano, 1970), the state space approach (Brogan, 1985), the power series expansion approach, i.e. the Frobenius method (Frobenius, 1873), the asymptotic expansion approach (Gol'denveizer, 1961) and the sampling surfaces (SaS) approach (Kulikov and Plotnikova, 2012a,b).

In the 3D shell formulation, the coefficients of the system of differential equations depend on the thickness coordinate. This fact restricts the implementation of the Pagano approach and the state space approach for the 3D exact solutions for layered shells. However, this restriction can be overcome in the case of artificial dividing the shell into a large number of individual layers through the layer thickness (Ye and Soldatos, 1994; Soldatos and Ye, 1995; Wu and Liu, 2007; Wu and Tsai, 2012) following a technique proposed by Soldatos and Hadjigeorgiou (1990). It is apparent that the analytical solutions derived by using such a technique are not exact, they are approximate. The most common approach to 3D exact solutions for layered shells is based on the Frobenius method (Srinivas, 1974; Ren, 1989; Varadan and Bhaskar, 1991; Huang and Tauchert, 1991; Chen and Shen, 1996; Heyliger, 1997; Wang and Zhong, 2003; Vel, 2011) or the modified Frobenius method (Burton and Noor, 1994; Xu and Noor, 1996; Kapuria et al., 1997a, 1997b, 1997c). The asymptotic approach has been also applied efficiently for the 3D stress analysis of layered shells (Tarn and Yen, 1995; Cheng and Reddy, 2002; Wu et al., 2005, 2007).

The SaS formulation was proposed by Kulikov and Plotnikova (2012b, 2013a, 2014a) for the 3D elastic analysis of homogeneous and layered shells. Next, it was extended to the electroelastic, thermoelastic and thermoelectroelastic analyses of layered shells (Kulikov and Plotnikova, 2013b, 2014b, c; Kulikov et al., 2015). According to this method, we choose I_n arbitrarily located SaS inside the nth layer parallel to the middle surface in order to introduce the displacements of these surfaces as basic shell unknowns, where $I_n \geq 3$. Such choice of unknowns with the consequent use of the Lagrange polynomials of degree $I_n - 1$ in the through-thickness approximations of displacements and strains of the nth layer leads to a very compact form of the governing equations of the SaS shell formulation.

An idea of the SaS concept can be traced back to contributions (Kulikov, 2001; Kulikov and Carrera, 2008) in which three, four and five equally spaced SaS are utilized. The SaS shell formulation with the arbitrary number of equispaced SaS is considered by Kulikov and Plotnikova (2011). The more general variational approach for layered shells with the SaS located at Chebyshev polynomial nodes (Bakhvalov, 1977) was developed later (Kulikov and Plotnikova, 2013a) because of the fact that the SaS formulation with equispaced SaS does not work properly with the higher-order Lagrange interpolation. The use of only Chebyshev polynomial nodes improves significantly the behavior of the higher-degree Lagrange polynomials because such a choice makes possible to minimize uniformly the error due to the Lagrange interpolation.

* Corresponding author.
E-mail address: gmkulikov@mail.ru (G.M. Kulikov).

http://dx.doi.org/10.1016/j.ijsolstr.2017.05.017
0020-7683/

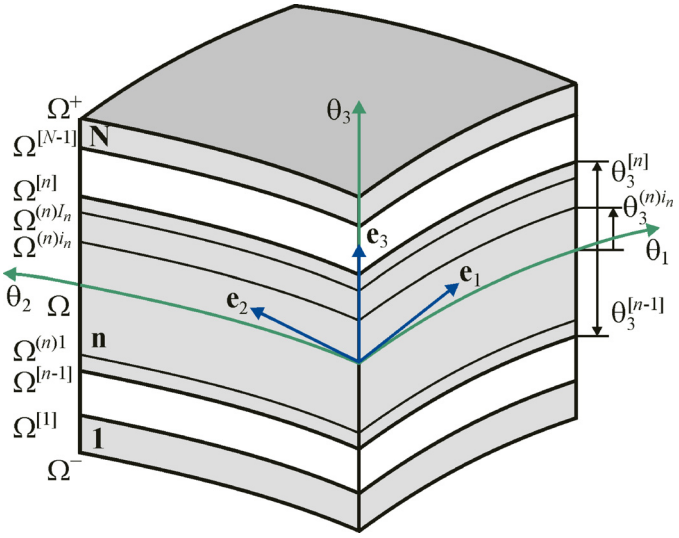

Fig. 1. Geometry of the layered shell.

This fact gives an opportunity to calculate the displacements and stresses with a prescribed accuracy employing the sufficiently large number of SaS. It means that the solutions based on the SaS concept asymptotically approach the 3D exact solutions of elasticity as the number of SaS tends to infinity. However, the implementation of the SaS variational formulation for layered shells (Kulikov and Plotnikova, 2013a) without using the interfaces is not possible. This restriction does not allow one to have all benefits of the higher-order Lagrange interpolation with Chebyshev polynomial nodes.

The present paper is intended to extend the SaS variational formulation to the strong SaS formulation for layered shells. The latter is based on the choice of all SaS inside the layers at Chebyshev polynomial nodes and integration of the equilibrium equations of elasticity. The use of interfaces is avoided that permits us to minimize uniformly the error due to the higher-order Lagrange interpolation. Thus, the strong SaS formulation can be applied efficiently to the obtaining of 3D solutions for layered composite shells.

2. Kinematic description of layered shell

Consider a layered shell of the thickness h. Let the middle surface Ω be described by orthogonal curvilinear coordinates θ_1 and θ_2, which are referred to the lines of principal curvatures of its surface. The coordinate θ_3 is oriented along the unit vector $\mathbf{e}_3(\theta_1,\theta_2)$ normal to the middle surface. Introduce the following notations: $\mathbf{e}_\alpha(\theta_1,\theta_2)$ are the orthonormal base vectors of the middle surface; $A_\alpha(\theta_1,\theta_2)$ are the coefficients of the first fundamental form; $k_\alpha(\theta_1,\theta_2)$ are the principal curvatures of the middle surface; $c_\alpha = 1 + k_\alpha\theta_3$ are the components of the shifter tensor; $c_\alpha^{(n)i_n}(\theta_1,\theta_2)$ are the components of the shifter tensor at SaS defined as

$$c_\alpha^{(n)i_n} = c_\alpha(\theta_3^{(n)i_n}) = 1 + k_\alpha\theta_3^{(n)i_n}, \tag{1}$$

where $\theta_3^{(n)i_n}$ are the transverse coordinates of SaS of the nth layer given by

$$\theta_3^{(n)i_n} = \frac{1}{2}(\theta_3^{[n-1]} + \theta_3^{[n]}) - \frac{1}{2}h_n\cos\left(\pi\frac{2i_n-1}{2I_n}\right), \tag{2}$$

where $\theta_3^{[n-1]}$ and $\theta_3^{[n]}$ are the transverse coordinates of interfaces $\Omega^{[n-1]}$ and $\Omega^{[n]}$ depicted in Fig. 1; $h_n = \theta_3^{[n]} - \theta_3^{[n-1]}$ is the thickness of the nth layer; the index n identifies the belonging of any quantity to the nth layer and runs from 1 to N, where N is the number of layers; the indices i_n and j_n, k_n to be introduced later identify the belonging of any quantity to the SaS of the nth layer and run from 1 to I_n; $N_{SaS} = I_1 + I_2 + \ldots + I_N$ is the total number of SaS.

In the orthonormal basis $\mathbf{e}_i$, the strains of the nth layer (Kulikov et al., 2015) can be written as

$$\begin{aligned} 2\varepsilon_{\alpha\beta}^{(n)} &= \tfrac{1}{c_\beta}\lambda_{\alpha\beta}^{(n)} + \tfrac{1}{c_\alpha}\lambda_{\beta\alpha}^{(n)}, \\ 2\varepsilon_{\alpha3}^{(n)} &= \tfrac{1}{c_\alpha}\lambda_{3\alpha}^{(n)} + u_{\alpha,3}^{(n)}, \quad \varepsilon_{33}^{(n)} = u_{3,3}^{(n)}, \end{aligned} \tag{3}$$

where $u_i^{(n)}$ and $\varepsilon_{ij}^{(n)}$ are the displacements and strains of the nth layer; $\lambda_{i\alpha}^{(n)}$ are the strain parameters of the nth layer expressed in terms of displacements as follows:

$$\begin{aligned} &\lambda_{\alpha\alpha}^{(n)} = \tfrac{1}{A_\alpha}u_{\alpha,\alpha}^{(n)} + B_\alpha u_\beta^{(n)} + k_\alpha u_3^{(n)}, \quad \lambda_{\beta\alpha}^{(n)} = \tfrac{1}{A_\alpha}u_{\beta,\alpha}^{(n)} - B_\alpha u_\alpha^{(n)} \\ &\text{for } \beta \neq \alpha, \\ &\lambda_{3\alpha}^{(n)} = \tfrac{1}{A_\alpha}u_{3,\alpha}^{(n)} - k_\alpha u_\alpha^{(n)}, \quad B_\alpha = \tfrac{1}{A_\alpha A_\beta}A_{\alpha,\beta} \quad \text{for } \beta \neq \alpha. \end{aligned} \tag{4}$$

Here and throughout this paper, Latin indices i, j, k, l range from 1 to 3, whereas Greek indices α, β range from 1 to 2; the symbol $(\ldots)_{,i}$ stands for the partial derivatives with respect to coordinates θ_i.

Introduce displacements of SaS of the nth layer $u_i^{(n)i_n}(\theta_1,\theta_2)$ as basic shell unknowns by

$$u_i^{(n)i_n} = u_i^{(n)}(\theta_3^{(n)i_n}). \tag{5}$$

The strains of SaS of the nth layer $\varepsilon_{ij}^{(n)i_n}(\theta_1,\theta_2)$ are defined as

$$\varepsilon_{ij}^{(n)i_n} = \varepsilon_{ij}^{(n)}(\theta_3^{(n)i_n}). \tag{6}$$

The use of Eqs. (3)–(6) leads to relations between the SaS variables

$$\begin{aligned} 2\varepsilon_{\alpha\beta}^{(n)i_n} &= \tfrac{1}{c_\beta^{(n)i_n}}\lambda_{\alpha\beta}^{(n)i_n} + \tfrac{1}{c_\alpha^{(n)i_n}}\lambda_{\beta\alpha}^{(n)i_n}, \\ 2\varepsilon_{\alpha3}^{(n)i_n} &= \tfrac{1}{c_\alpha^{(n)i_n}}\lambda_{3\alpha}^{(n)i_n} + \beta_\alpha^{(n)i_n}, \quad \varepsilon_{33}^{(n)i_n} = \beta_3^{(n)i_n}, \end{aligned} \tag{7}$$

where $\lambda_{i\alpha}^{(n)i_n}(\theta_1,\theta_2)$ are the strain parameters of SaS of the nth layer; $\beta_i^{(n)i_n}(\theta_1,\theta_2)$ are the values of the derivative of displacements with respect to thickness coordinate at SaS given by

$$\begin{aligned} \lambda_{\alpha\alpha}^{(n)i_n} &= \lambda_{\alpha\alpha}^{(n)}(\theta_3^{(n)i_n}) = \tfrac{1}{A_\alpha}u_{\alpha,\alpha}^{(n)i_n} + B_\alpha u_\beta^{(n)i_n} + k_\alpha u_3^{(n)i_n} \quad \text{for } \beta \neq \alpha, \\ \lambda_{\beta\alpha}^{(n)i_n} &= \lambda_{\beta\alpha}^{(n)}(\theta_3^{(n)i_n}) = \tfrac{1}{A_\alpha}u_{\beta,\alpha}^{(n)i_n} - B_\alpha u_\alpha^{(n)i_n} \quad \text{for } \beta \neq \alpha \\ \lambda_{3\alpha}^{(n)i_n} &= \lambda_{3\alpha}^{(n)}(\theta_3^{(n)i_n}) = \tfrac{1}{A_\alpha}u_{3,\alpha}^{(n)i_n} - k_\alpha u_\alpha^{(n)i_n}, \end{aligned} \tag{8}$$

$$\beta_i^{(n)i_n} = u_{i,3}^{(n)}(\theta_3^{(n)i_n}). \tag{9}$$

Up to this moment no assumptions concerning the displacement field have been made. We start now with the first assumption of the SaS formulation for layered shells. Let us assume that the displacements are distributed through the thickness of the nth layer in the following form:

$$u_i^{(n)} = \sum_{i_n} L^{(n)i_n}u_i^{(n)i_n}, \tag{10}$$

where $L^{(n)i_n}(\theta_3)$ are the Lagrange basis polynomials of degree $I_n - 1$ expressed as

$$L^{(n)i_n} = \prod_{j_n \neq i_n}\frac{\theta_3 - \theta_3^{(n)j_n}}{\theta_3^{(n)i_n} - \theta_3^{(n)j_n}}. \tag{11}$$

Substitution of the SaS interpolation (10) in Eq. (9) results in

$$\beta_i^{(n)i_n} = \sum_{j_n} M^{(n)j_n}(\theta_3^{(n)i_n})u_i^{(n)j_n}, \tag{12}$$

where $M^{(n)j_n} = L_3^{(n)j_n}$ are the derivatives of the Lagrange basis polynomials, which are calculated at SaS as follows:

$$M^{(n)j_n}(\theta_3^{(n)i_n}) = \frac{1}{\theta_3^{(n)j_n} - \theta_3^{(n)i_n}} \prod_{k_n \neq i_n,\, j_n} \frac{\theta_3^{(n)i_n} - \theta_3^{(n)k_n}}{\theta_3^{(n)j_n} - \theta_3^{(n)k_n}} \quad \text{for } j_n \neq i_n,$$
$$M^{(n)i_n}(\theta_3^{(n)i_n}) = -\sum_{j_n \neq i_n} M^{(n)j_n}(\theta_3^{(n)i_n}). \tag{13}$$

It is seen from Eq. (12) that the key functions $\beta_i^{(n)i_n}$ of the SaS shell formulation are represented as a linear combination of displacements of SaS of the nth layer $u_i^{(n)j_n}$.

Remark 1. The functions $\beta_i^{(n)1}, \beta_i^{(n)2}, \ldots, \beta_i^{(n)I_n}$ are linearly dependent, that is, there exist numbers $\alpha^{(n)1}, \alpha^{(n)2}, \ldots, \alpha^{(n)I_n}$, which are not all zero such that

$$\sum_{i_n} \alpha^{(n)i_n} \beta_i^{(n)i_n} = 0. \tag{14}$$

The proof of this statement for layered plates can be found in Kulikov and Plotnikova (2016). The extension to layered shells is straightforward.

The following step consists in a choice of the suitable approximation of strains through the thickness of the nth layer. It is apparent that the strain distribution should be chosen similar to the displacement distribution (10). Therefore, the strains are distributed through the thickness of the nth layer as follows:

$$\varepsilon_{ij}^{(n)} = \sum_{i_n} L^{(n)i_n} \varepsilon_{ij}^{(n)i_n}. \tag{15}$$

As can be seen, the strains (15) explicitly depend on the SaS strains of the nth layer $\varepsilon_{ij}^{(n)i_n}$ defined by Eqs. (7), (8) and (12). This fact allows one to represent the governing equations of the SaS shell formulation in a very compact form.

Remark 2. It is worth noting that in the SaS plate formulation (Kulikov and Plotnikova, 2012a) the strain approximation (15) is dependent and follows from the displacement approximation (10) directly. On the contrary, in the SaS shell formulation the through-thickness strain distribution is introduced independently because of varying the shifter tensor in the thickness direction.

Remark 3. Strain-displacement relationships (7) and (15) exactly represent rigid-body motions of a layered shell in any curvilinear coordinate system. This statement can be proved via a technique developed by Kulikov and Plotnikova (2013a), where the weak SaS formulation for layered shells is considered.

3. Strong SaS formulation for layered shell

For simplicity, we consider the case of linear elastic materials, which are described by

$$\sigma_{ij}^{(n)} = C_{ijkl}^{(n)} \varepsilon_{kl}^{(n)}, \tag{16}$$

where $C_{ijkl}^{(n)}$ are the elastic constants of the nth layer. Here and in the following developments, the summation on repeated Latin indices is implied.

The equilibrium equations of the layered shell (Ambartsumyan, 1964) can be expressed as

$$\frac{1}{c_\alpha}\mu_{\alpha\alpha}^{(n)} + \frac{1}{c_\beta}\mu_{\alpha\beta}^{(n)} + \sigma_{\alpha 3,3}^{(n)} = 0 \quad \text{for } \beta \neq \alpha,$$
$$\frac{1}{c_1}\mu_{31}^{(n)} + \frac{1}{c_2}\mu_{32}^{(n)} + \sigma_{33,3}^{(n)} = 0, \tag{17}$$

where $\sigma_{ij}^{(n)}$ are the stresses of the nth layer; $\mu_{i\alpha}^{(n)}$ are the stress parameters of the nth layer given by

$$\mu_{\alpha\alpha}^{(n)} = \frac{1}{A_\alpha}\sigma_{\alpha\alpha,\alpha}^{(n)} + 2B_\alpha\sigma_{\alpha\beta}^{(n)} + 2k_\alpha\sigma_{\alpha 3}^{(n)} \quad \text{for } \beta \neq \alpha,$$
$$\mu_{\beta\alpha}^{(n)} = \frac{1}{A_\alpha}\sigma_{\beta\alpha,\alpha}^{(n)} + B_\alpha(\sigma_{\beta\beta}^{(n)} - \sigma_{\alpha\alpha}^{(n)}) + k_\alpha\sigma_{\beta 3}^{(n)} \quad \text{for } \beta \neq \alpha, \tag{18}$$
$$\mu_{3\alpha}^{(n)} = \frac{1}{A_\alpha}\sigma_{\alpha 3,\alpha}^{(n)} + B_\alpha\sigma_{\beta 3}^{(n)} - k_\alpha(\sigma_{\alpha\alpha}^{(n)} - \sigma_{33}^{(n)}) \quad \text{for } \beta \neq \alpha.$$

The boundary conditions on the bottom and top surfaces are defined as

$$u_i^{(1)}(-h/2) = w_i^- \quad \text{or} \quad \sigma_{i3}^{(1)}(-h/2) = p_i^-, \tag{19}$$

$$u_i^{(N)}(h/2) = w_i^+ \quad \text{or} \quad \sigma_{i3}^{(N)}(h/2) = p_i^+, \tag{20}$$

where $w_i^-(\theta_1, \theta_2)$ and $w_i^+(\theta_1, \theta_2)$ are the prescribed displacements; $p_i^-(\theta_1, \theta_2)$ and $p_i^+(\theta_1, \theta_2)$ are the external mechanical loads acting on the bottom and top surfaces.

The continuity conditions at interfaces are

$$u_i^{(m)}(\theta_3^{[m]}) = u_i^{(m+1)}(\theta_3^{[m]}), \tag{21}$$

$$\sigma_{i3}^{(m)}(\theta_3^{[m]}) = \sigma_{i3}^{(m+1)}(\theta_3^{[m]}), \tag{22}$$

where the index m identifies the belonging of any quantity to the interface $\Omega^{[m]}$ and runs from 1 to $N-1$.

Following the SaS technique, we introduce stresses at the SaS of the nth layer $\sigma_{ij}^{(n)i_n}(\theta_1, \theta_2)$ as

$$\sigma_{ij}^{(n)i_n} = \sigma_{ij}^{(n)}(\theta_3^{(n)i_n}). \tag{23}$$

According to Eqs. (6), (16) and (23) the constitutive equations can be written in terms of SaS variables as

$$\sigma_{ij}^{(n)i_n} = C_{ijkl}^{(n)} \varepsilon_{kl}^{(n)i_n}. \tag{24}$$

The use of Eqs. (15), (16) and (24) leads to the distribution of stresses through the thickness of the nth layer

$$\sigma_{ij}^{(n)} = \sum_{i_n} L^{(n)i_n} \sigma_{ij}^{(n)i_n}. \tag{25}$$

Satisfying the equilibrium Eqs. (17) at inner points $\theta_3^{(n)m_n}$ throughout the layers, the following differential equations are obtained:

$$\frac{1}{c_\alpha^{(n)m_n}}\mu_{\alpha\alpha}^{(n)m_n} + \frac{1}{c_\beta^{(n)m_n}}\mu_{\alpha\beta}^{(n)m_n} + \gamma_\alpha^{(n)m_n} = 0 \quad \text{for } \beta \neq \alpha,$$
$$\frac{1}{c_1^{(n)m_n}}\mu_{31}^{(n)m_n} + \frac{1}{c_2^{(n)m_n}}\mu_{32}^{(n)m_n} + \gamma_3^{(n)m_n} = 0, \tag{26}$$

where $\mu_{i\alpha}^{(n)m_n}$ are the stress parameters at SaS of the nth layer given by

$$\mu_{\alpha\alpha}^{(n)m_n} = \mu_{\alpha\alpha}^{(n)}(\theta_3^{(n)m_n}) = \frac{1}{A_\alpha}\sigma_{\alpha\alpha,\alpha}^{(n)m_n} + 2B_\alpha\sigma_{\alpha\beta}^{(n)m_n} + 2k_\alpha\sigma_{\alpha 3}^{(n)m_n} \quad \text{for } \beta \neq \alpha,$$
$$\mu_{\beta\alpha}^{(n)m_n} = \mu_{\beta\alpha}^{(n)}(\theta_3^{(n)m_n}) = \frac{1}{A_\alpha}\sigma_{\beta\alpha,\alpha}^{(n)m_n} + B_\alpha(\sigma_{\beta\beta}^{(n)m_n} - \sigma_{\alpha\alpha}^{(n)m_n}) + k_\alpha\sigma_{\beta 3}^{(n)m_n} \quad \text{for } \beta \neq \alpha, \tag{27}$$
$$\mu_{3\alpha}^{(n)m_n} = \mu_{3\alpha}^{(n)}(\theta_3^{(n)m_n}) = \frac{1}{A_\alpha}\sigma_{\alpha 3,\alpha}^{(n)m_n} + B_\alpha\sigma_{\beta 3}^{(n)m_n} - k_\alpha(\sigma_{\alpha\alpha}^{(n)m_n} - \sigma_{33}^{(n)m_n}) \quad \text{for } \beta \neq \alpha,$$

$$\gamma_i^{(n)m_n} = \sigma_{i3,3}^{(n)}(\theta_3^{(n)m_n}) = \sum_{i_n} M^{(n)i_n}(\theta_3^{(n)m_n})\sigma_{i3}^{(n)i_n}, \tag{28}$$

where $m_n = 2, 3, \ldots, I_n - 1$; this index identifies the belonging of any quantity to the inner SaS of the nth layer.

Next, we satisfy the boundary conditions (19) and (20):

$$\sum_{i_1} L^{(1)i_1}(-h/2)u_i^{(1)i_1} = w_i^- \quad \text{or} \quad \sum_{i_1} L^{(1)i_1}(-h/2)\sigma_{i3}^{(1)i_1} = p_i^-, \tag{29}$$

$$\sum_{i_N} L^{(N)i_N}(h/2)u_i^{(N)i_N} = w_i^+ \quad \text{or} \quad \sum_{i_N} L^{(N)i_N}(h/2)\sigma_{i3}^{(N)i_N} = p_i^+, \tag{30}$$

and the continuity conditions (21) and (22) that result in

$$\sum_{i_m} L^{(m)i_m}(\theta_3^{[m]})u_i^{(m)i_m} = \sum_{i_{m+1}} L^{(m+1)i_{m+1}}(\theta_3^{[m]})u_i^{(m+1)i_{m+1}}, \tag{31}$$

$$\sum_{i_m} L^{(m)i_m}(\theta_3^{[m]})\sigma_{i3}^{(m)i_m} = \sum_{i_{m+1}} L^{(m+1)i_{m+1}}(\theta_3^{[m]})\sigma_{i3}^{(m+1)i_{m+1}}. \tag{32}$$

Thus, the proposed strong shell formulation deals with $3(I_1+I_2+...+I_N)$ governing Eqs. (26), (29)–(32) for finding the same number of SaS displacements $u_i^{(n)i_n}$. These differential and algebraic equations have to be solved to describe the response of the layered shell with different boundary conditions. For this purpose, the differential quadrature method (Shu, 2000; Tornabene et al., 2015) could be applied effectively. Here, however, we restrict ourselves to 3D exact solutions for the simply supported layered cylindrical shells and panels to assess the potential of the strong SaS formulation developed. The general boundary conditions will be discussed in our future developments.

4. Analytical solution for simply supported layered cylindrical shell

In this section, we study the simply supported layered cylindrical shell of the radius R subjected to the sinusoidally distributed transverse load acting on the bottom surface

$$p_3^- = p_{30}^- \sin\bar{r}\theta_1 \cos s\theta_2, \quad \bar{r} = r\pi/L \tag{33}$$

or imposed transverse deformation

$$w_3^- = w_{30}^- \sin\bar{r}\theta_1 \cos s\theta_2, \tag{34}$$

where L is the length of the shell; θ_1 and θ_2 are the axial and circumferential coordinates of the middle surface; r, s are the wave numbers.

The edge boundary conditions are written as

$$\sigma_{11}^{(n)} = u_2^{(n)} = u_3^{(n)} = 0 \text{ at } \theta_1 = 0 \text{ and } \theta_1 = L. \tag{35}$$

To satisfy boundary conditions (35), we seek the analytical solution in the following form:

$$\begin{aligned} &u_1^{(n)i_n} = u_{10}^{(n)i_n}\cos\bar{r}\theta_1\cos s\theta_2, \quad u_2^{(n)i_n} = u_{20}^{(n)i_n}\sin\bar{r}\theta_1\sin s\theta_2,\\ &u_3^{(n)i_n} = u_{30}^{(n)i_n}\sin\bar{r}\theta_1\cos s\theta_2. \end{aligned} \tag{36}$$

The use of Eqs. (7), (8), (12), (24) and (36) yields

$$\begin{aligned} &(\varepsilon_{11}^{(n)i_n},\ \sigma_{11}^{(n)i_n}) = (\varepsilon_{110}^{(n)i_n},\ \sigma_{110}^{(n)i_n})\sin\bar{r}\theta_1\cos s\theta_2, \quad (\varepsilon_{22}^{(n)i_n},\ \sigma_{22}^{(n)i_n})\\ &\quad = (\varepsilon_{220}^{(n)i_n},\ \sigma_{220}^{(n)i_n})\sin\bar{r}\theta_1\cos s\theta_2,\\ &(\varepsilon_{12}^{(n)i_n},\ \sigma_{12}^{(n)i_n}) = (\varepsilon_{120}^{(n)i_n},\ \sigma_{120}^{(n)i_n})\cos\bar{r}\theta_1\sin s\theta_2, \quad (\varepsilon_{13}^{(n)i_n},\ \sigma_{13}^{(n)i_n})\\ &\quad = (\varepsilon_{130}^{(n)i_n},\ \sigma_{130}^{(n)i_n})\cos\bar{r}\theta_1\cos s\theta_2,\\ &(\varepsilon_{23}^{(n)i_n},\ \sigma_{23}^{(n)i_n}) = (\varepsilon_{230}^{(n)i_n},\ \sigma_{230}^{(n)i_n})\sin\bar{r}\theta_1\sin s\theta_2, \quad (\varepsilon_{33}^{(n)i_n},\ \sigma_{33}^{(n)i_n})\\ &\quad = (\varepsilon_{330}^{(n)i_n},\ \sigma_{330}^{(n)i_n})\sin\bar{r}\theta_1\cos s\theta_2, \end{aligned} \tag{37}$$

where

$$\begin{aligned} &\varepsilon_{110}^{(n)i_n} = -\bar{r}u_{10}^{(n)i_n}, \quad \varepsilon_{220}^{(n)i_n} = \tfrac{1}{\varsigma^{(n)i_n}}(su_{20}^{(n)i_n} + u_{30}^{(n)i_n}),\\ &2\varepsilon_{120}^{(n)i_n} = -\tfrac{s}{\varsigma^{(n)i_n}}u_{10}^{(n)i_n} + \bar{r}u_{20}^{(n)i_n},\\ &2\varepsilon_{130}^{(n)i_n} = \bar{r}u_{30}^{(n)i_n} + \beta_{10}^{(n)i_n}, \quad 2\varepsilon_{230}^{(n)i_n} = -\tfrac{1}{\varsigma^{(n)i_n}}(su_{30}^{(n)i_n} + u_{20}^{(n)i_n}) + \beta_{20}^{(n)i_n},\\ &\varepsilon_{330}^{(n)i_n} = \beta_{30}^{(n)i_n},\\ &\beta_{i0}^{(n)i_n} = \sum_{j_n} M^{(n)j_n}(\theta_3^{(n)i_n})u_{i0}^{(n)j_n}, \quad \varsigma^{(n)i_n} = R + \theta_3^{(n)i_n}. \end{aligned} \tag{38}$$

Considering a special case of the orthotropic material with

$$\begin{aligned} C_{1112}^{(n)} = C_{1113}^{(n)} = C_{1123}^{(n)} = C_{2212}^{(n)} = C_{2213}^{(n)} = C_{2223}^{(n)} = C_{1213}^{(n)} = C_{1223}^{(n)}\\ = C_{1233}^{(n)} = C_{1323}^{(n)} = C_{1333}^{(n)} = C_{2333}^{(n)} = 0, \end{aligned}$$

one can write the constitutive equations in a compact form as

$$\sigma_{ij0}^{(n)i_n} = C_{ijkl}^{(n)}\varepsilon_{kl0}^{(n)i_n}. \tag{39}$$

Substituting (36) and (37) in Eqs. (26), (29)–(32), we arrive at the system of linear equations

$$\begin{aligned} &\bar{r}\sigma_{110}^{(n)m_n} + \frac{1}{\varsigma^{(n)m_n}}(s\sigma_{120}^{(n)m_n} + \sigma_{130}^{(n)m_n}) + \sum_{i_n} M^{(n)i_n}(\theta_3^{(n)m_n})\sigma_{130}^{(n)i_n} = 0,\\ &-\bar{r}\sigma_{120}^{(n)m_n} - \frac{1}{\varsigma^{(n)m_n}}(s\sigma_{220}^{(n)m_n} - 2\sigma_{230}^{(n)m_n}) + \sum_{i_n} M^{(n)i_n}(\theta_3^{(n)m_n})\sigma_{230}^{(n)i_n} = 0,\\ &-\bar{r}\sigma_{130}^{(n)m_n} + \frac{1}{\varsigma^{(n)m_n}}(s\sigma_{230}^{(n)m_n} - \sigma_{220}^{(n)m_n} + \sigma_{330}^{(n)m_n})\\ &\quad + \sum_{i_n} M^{(n)i_n}(\theta_3^{(n)m_n})\sigma_{330}^{(n)i_n} = 0, \end{aligned} \tag{40}$$

$$\begin{aligned} &\sum_{i_1} L^{(1)i_1}(-h/2)\sigma_{130}^{(1)i_1} = 0, \quad \sum_{i_1} L^{(1)i_1}(-h/2)\sigma_{230}^{(1)i_1} = 0,\\ &\sum_{i_1} L^{(1)i_1}(-h/2)u_{30}^{(1)i_1} = w_{30}^- \quad \text{or} \quad \sum_{i_1} L^{(1)i_1}(-h/2)\sigma_{330}^{(1)i_1} = p_{30}^-, \end{aligned} \tag{41}$$

$$\sum_{i_N} L^{(N)i_N}(h/2)\sigma_{i30}^{(N)i_N} = 0, \tag{42}$$

$$\sum_{i_m} L^{(m)i_m}(\theta_3^{[m]})u_{i0}^{(m)i_m} = \sum_{i_{m+1}} L^{(m+1)i_{m+1}}(\theta_3^{[m]})u_{i0}^{(m+1)i_{m+1}}, \tag{43}$$

$$\sum_{i_m} L^{(m)i_m}(\theta_3^{[m]})\sigma_{i30}^{(m)i_m} = \sum_{i_{m+1}} L^{(m+1)i_{m+1}}(\theta_3^{[m]})\sigma_{i30}^{(m+1)i_{m+1}} \tag{44}$$

of order $3(I_1+I_2+...+I_N)$. Therefore, the SaS displacement amplitudes of the nth layer $u_{i0}^{(n)i_n}$ can be found with the Symbolic Math Toolbox, which incorporates symbolic computations into the numeric environment of MATLAB. For the solution of the system of algebraic Eqs. (40)–(44) the function *solve* is utilized. This makes it possible to obtain the analytical solution for layered orthotropic cylindrical shells in the framework of the strong SaS formulation.

5. Numerical examples

Here, we study simply supported cross-ply composite cylindrical shells under sinusoidally distributed transverse loading

$$p_3^- = -p_0 \sin\frac{\pi\theta_1}{L}\cos 4\theta_2 \tag{45}$$

or imposed transverse deformation

$$w_3^- = w_0 \sin\frac{\pi\theta_1}{L}\cos 4\theta_2. \tag{46}$$

5.1. Two-layer cross-ply cylindrical shell

Consider first a two-layer cylindrical shell composed of the graphite-epoxy composite with the stacking sequence [0/90], that is, the fiber direction coincides with the axial direction in a bottom layer and the circumferential direction in a top layer. The material properties of the graphite-epoxy are taken to be $E_L = 25E_T$, $G_{LT} = 0.5E_T$, $G_{TT} = 0.2E_T$, $E_T = 10^6$ and $\nu_{LT} = \nu_{TT} = 0.25$. The geometric parameters of the shell are $h_1 = h_2 = h/2$ and $L/R = 4$.

Table 1
Results of the convergence study for a two-ply cylindrical shell with $a/h=4$ under transverse loading.

I_n	$\bar{u}_3(0)$	$\bar{\sigma}_{11}(0.5)$	$\bar{\sigma}_{12}(0.5)$	$\bar{\sigma}_{13}(-0.25)$	$\bar{\sigma}_{23}(0.25)$	$\bar{\sigma}_{33}(0.25)$
5	0.627456109834797	0.222402480080094	2.08282677245192	2.82825683116275	−4.51196969231450	−0.694921544890055
7	0.610534559073471	0.212286721374066	2.00936803590992	2.76095019701703	−4.43996861878763	−0.695982262741641
9	0.609966478690596	0.211952419198707	2.00698829803498	2.75831965062111	−4.43974087338684	−0.696649460360477
11	0.609954179197583	0.211945246559437	2.00693821568360	2.75825972852904	−4.43969445712463	−0.696663267722788
13	0.609953983794841	0.211945132166869	2.00693742854060	2.75825876454161	−4.43969417393375	−0.696663625886105
15	0.609953981395686	0.211945130750316	2.00693741887292	2.75825875266880	−4.43969416538568	−0.696663629459429
17	0.609953981372326	0.211945130736414	2.00693741877849	2.75825875255318	−4.43969416534211	−0.696663629502759
19	**0.60995398137213**9	**0.21194513073630**3	**2.00693741877773**	**2.75825875255226**	**−4.43969416534148**	**−0.69666362950304**6
21	0.609953981372138	0.211945130736302	2.00693741877773	2.75825875255226	−4.43969416534148	−0.696663629503049
Varadan and Bhaskar (1991)	0.6100	0.2120	2.007	2.758	−4.440	−0.70

Table 2
Results of the convergence study for a two-ply cylindrical shell with $a/h=10$ under transverse loading.

I_n	$\bar{u}_3(0)$	$\bar{\sigma}_{11}(0.5)$	$\bar{\sigma}_{12}(0.5)$	$\bar{\sigma}_{13}(-0.25)$	$\bar{\sigma}_{23}(0.25)$	$\bar{\sigma}_{33}(0.25)$
5	0.336472196399464	0.195298456073440	1.26084767027714	1.60731843656651	−5.47159780042336	−1.67804070744202
7	0.332989669138597	0.193022871004216	1.24681951936033	1.59093305663804	−5.45739134674453	−1.67989048928871
9	0.332966275322987	0.193007699871106	1.24672633450084	1.59081443264255	−5.45739394038181	−1.67997311591832
11	0.332966183227366	0.193007640335065	1.24672597044009	1.59081395655357	−5.45739360318423	−1.67997340269310
13	0.332966182970104	0.193007640168589	1.24672596942568	1.59081395521749	−5.45739360288912	−1.67997340395275
15	**0.33296618296955**7	**0.19300764016823**4	**1.24672596942352**	**1.59081395521464**	**−5.45739360288723**	**−1.67997340395488**
17	0.332966182969556	0.193007640168233	1.24672596942352	1.59081395521462	−5.45739360288723	−1.67997340395489
Varadan and Bhaskar (1991)	0.3330	0.1930	1.247	1.591	−5.457	−1.68

Table 3
Results of the convergence study for a two-ply cylindrical shell with $a/h=4$ under imposed transverse deformation.

I_n	$\bar{u}_3(0.5)$	$\bar{\sigma}_{11}(0.5)$	$\bar{\sigma}_{12}(0.5)$	$\bar{\sigma}_{13}(-0.25)$	$\bar{\sigma}_{23}(0.25)$	$\bar{\sigma}_{33}(0.25)$
5	0.913414424999229	0.849605098798578	0.79566569813073	1.08042923963906	−17.2362846620889	−2.65468661856176
7	0.909084738271330	0.831356157820356	0.78690766863254	1.08124188496975	−17.3877820895545	−2.72560212960496
9	0.908913648934416	0.830752000760533	0.78664331853293	1.08112923511494	−17.4016584824474	−2.73053232990295
11	0.908909508082020	0.830739187192274	0.78663817618318	1.08112565964097	−17.4017970422349	−2.73063673835422
13	0.908909439009414	0.830738982069839	0.78663809799181	1.08112559836309	−17.4018010276891	−2.73063894177125
15	0.908909438151820	0.830738979505863	0.78663809703217	1.08112559759846	−17.4018010567819	−2.73063896559990
17	0.908909438143473	0.830738979480485	0.78663809702272	1.08112559759103	−17.4018010572210	−2.73063896586542
19	**0.90890943814340**7	**0.83073897948027**9	**0.78663809702264**	**1.08112559759097**	**−17.401801057223**3	**−2.73063896586731**
21	0.908909438143406	0.830738979480278	0.78663809702264	1.08112559759097	−17.4018010572234	−2.73063896586732

In the case of transverse loading (45), we utilize the dimensionless variables as functions of the thickness coordinate:

$$\begin{aligned}
&\bar{\sigma}_{11}=10h^2\sigma_{11}(L/2,\ 0,\ z)/R^2p_0, \quad \bar{\sigma}_{22}=h^2\sigma_{22}(L/2,\ 0,\ z)/R^2p_0,\\
&\bar{\sigma}_{12}=100h^2\sigma_{12}(0,\ \pi/8,\ z)/R^2p_0, \quad \bar{\sigma}_{13}=100h\sigma_{13}(0,\ 0,\ z)/Rp_0,\\
&\bar{\sigma}_{23}=10h\sigma_{23}(L/2,\ \pi/8,\ z)/Rp_0, \quad \bar{\sigma}_{33}=\sigma_{33}(L/2,\ 0,\ z)/p_0,\\
&\bar{u}_1=E_Lh^2u_1(0,\ 0,\ z)/R^3p_0, \quad \bar{u}_2=E_Lh^3u_2(L/2,\ \pi/8,\ z)/R^4p_0,\\
&\bar{u}_3=E_Lh^3u_3(L/2,\ 0,\ z)/R^4p_0, \quad z=\theta_3/h,
\end{aligned} \tag{47}$$

where $p_0=1$ and $R=1$, whereas the case of imposed transverse deformation (46) is characterized by the following dimensionless variables:

$$\begin{aligned}
&\bar{\sigma}_{11}=100R\sigma_{11}(L/2,\ 0,\ z)/E_Lw_0, \quad \bar{\sigma}_{22}=10R\sigma_{22}(L/2,\ 0,\ z)/E_Lw_0,\\
&\bar{\sigma}_{12}=100R\sigma_{12}(0,\ \pi/8,\ z)/E_Lw_0, \quad \bar{\sigma}_{13}=100R^2\sigma_{13}(0,\ 0,\ z)/hE_Lw_0,\\
&\bar{\sigma}_{23}=100R^2\sigma_{23}(L/2,\ \pi/8,\ z)/hE_Lw_0,\\
&\bar{\sigma}_{33}=10R^3\sigma_{33}(L/2,\ 0,\ z)/h^2E_Lw_0,\\
&\bar{u}_1=100u_1(0,\ 0,\ z)/w_0, \quad \bar{u}_2=10u_2(L/2,\ \pi/8,\ z)/w_0,\\
&\bar{u}_3=u_3(L/2,\ 0,\ z)/w_0,
\end{aligned} \tag{48}$$

where $w_0=1$.

Tables 1–4 list the results of the convergence study due to increasing the number of SaS I_n inside each layer for two values of the slenderness ratio R/h. The SaS analytical solution for a two-ply cylindrical shell under transverse loading is compared with the exact solution (Varadan and Bhaskar, 1991). As it turned out, the developed algorithm of symbolic computations provides already 14 right digits for all basic variables at crucial points since 19 and 15 SaS respectively for thick and moderately thick shells. However, the use of the more number of SaS does not lead to a better accuracy. This is due to the fact that the authors restrict themselves to default precision that provides roughly from 15 to 16 decimal digits of precision. Note also that we did not discover the divergence of the developed algorithm of symbolic computations even in the case of using more than 50 SaS.

Figs. 2 and 3 show the distributions of displacements and stresses in the thickness direction for different slenderness ratios by choosing nine SaS for both layers. These results demonstrate the high potential of the strong SaS formulation because the boundary conditions on bottom and top surfaces and the continuity conditions at interfaces for the transverse stresses are satisfied exactly. It should be noted that in a variational SaS shell formulation (Kulikov and Plotnikova, 2013a) the boundary conditions on outer surfaces and the continuity conditions at interfaces are satisfied approximately.

5.2. Three-layer cross-ply cylindrical shell

Next, we consider a symmetric three-layer cylindrical shell made of the graphite-epoxy composite with the stacking sequence [90/0/90], that is, the fiber directions coincide with θ_2-direction in outer layers and θ_1-direction in a central layer. The material properties of the graphite-epoxy are given in a previous section. The geometric parameters of the shell are taken to be $h_1=h_2=h_3=h/3$ and $L/R=4$.

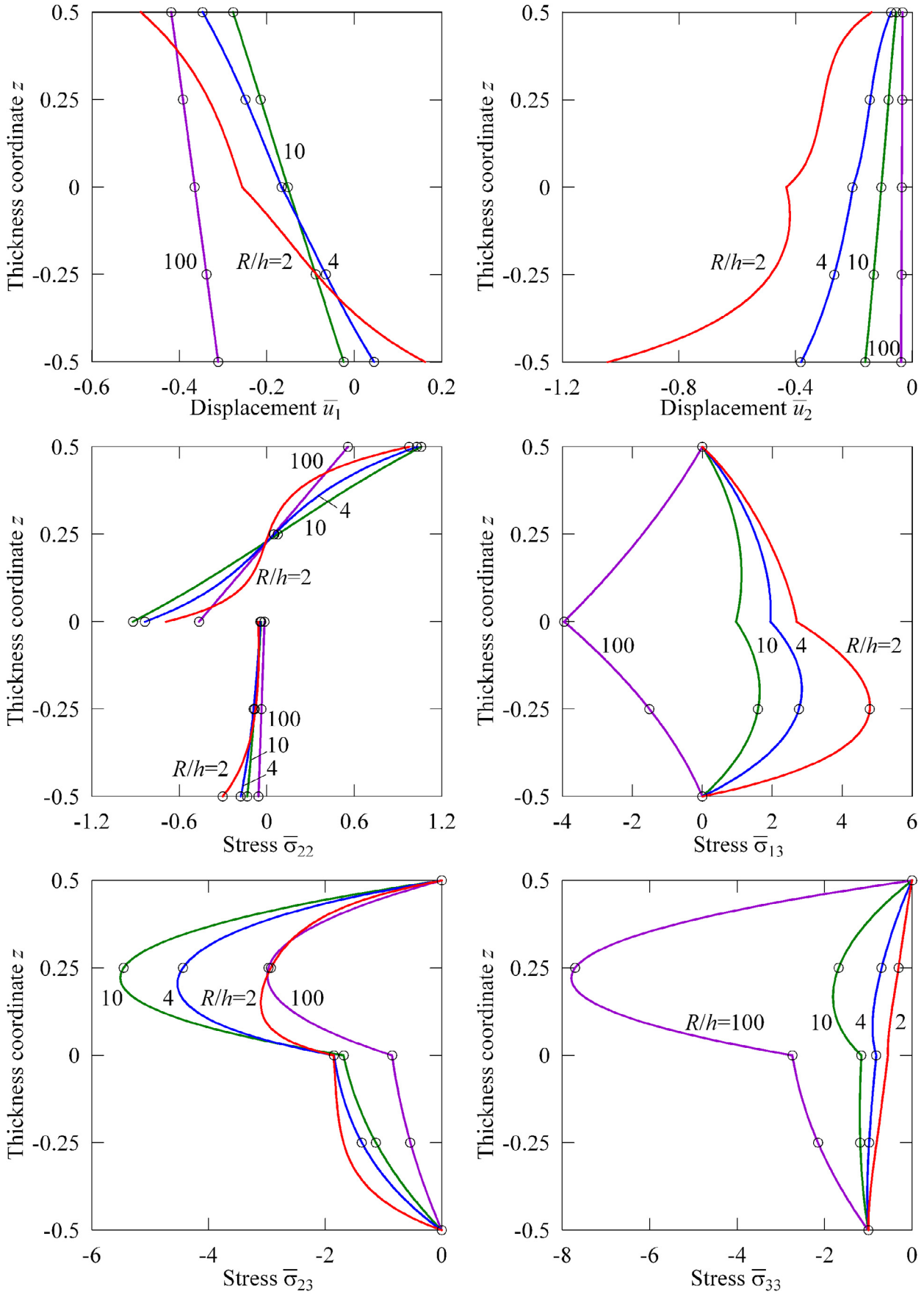

Fig. 2. Through-thickness distributions of displacements and stresses for a two-ply cylindrical shell under transverse loading for $l_1 = l_2 = 9$: SaS formulation (—) and Varadan-Bhaskar exact solution (○).

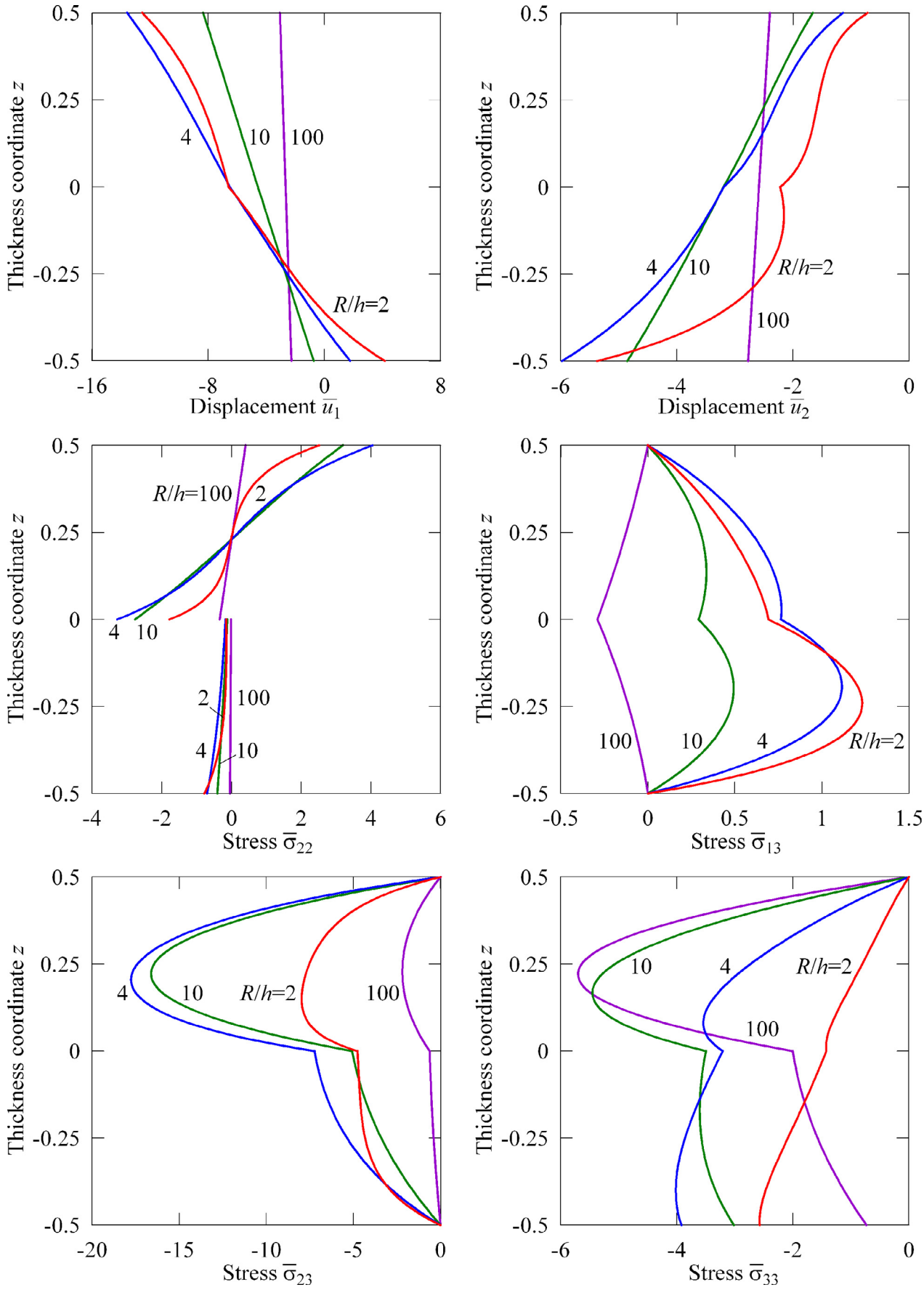

Fig. 3. Through-thickness distributions of displacements and stresses for a two-ply cylindrical shell under imposed transverse deformation for $I_1 = I_2 = 9$.

Table 4
Results of the convergence study for a two-ply cylindrical shell with $a/h=10$ under imposed transverse deformation.

I_n	$\bar{u}_3(0.5)$	$\bar{\sigma}_{11}(0.5)$	$\bar{\sigma}_{12}(0.5)$	$\bar{\sigma}_{13}(-0.25)$	$\bar{\sigma}_{23}(0.25)$	$\bar{\sigma}_{33}(0.25)$
5	0.997903138881139	0.582442004049350	0.376024807692806	0.479353390785245	−16.3180418949764	−5.00445017420616
7	0.997775691228728	0.581647600587627	0.375711737178500	0.479405570062649	−16.4450905003496	−5.06211656298187
9	0.997774710147125	0.581642560364331	0.375709931654008	0.479403350376521	−16.4462484477059	−5.06271959687891
11	0.997774705918184	0.581642541094385	0.375709925387547	0.479403338899911	−16.4462519597553	−5.06272185503671
13	0.997774705905915	0.581642541040064	0.375709925370822	0.479403338866002	−16.4462519715156	−5.06272186272670
15	**0.997774705905889**	**0.581642541039946**	**0.375709925370786**	**0.479403338865928**	**−16.4462519715367**	**−5.06272186274140**
17	0.997774705905889	0.581642541039945	0.375709925370786	0.479403338865925	−16.4462519715368	−5.06272186274143

Table 5
Results of the convergence study for a symmetric three-ply cylindrical shell with $a/h=10$ under transverse loading.

I_n	$\bar{u}_3(0)$	$\bar{\sigma}_{11}(0.5)$	$\bar{\sigma}_{12}(0.5)$	$\bar{\sigma}_{13}(-1/6)$	$\bar{\sigma}_{23}(0)$	$\bar{\sigma}_{33}(0)$
5	0.122462862407215	0.074018613130080	0.374341658226684	0.827155208074006	−3.26775914476089	−1.27136083305538
7	0.122329564274619	0.073922458401339	0.373901435494128	0.826374300048013	−3.26358717508330	−1.27016468921926
9	0.122329111894357	0.073922149301315	0.373900041197308	0.826371745504328	−3.26357270543907	−1.27016014796717
11	0.122329110998409	0.073922148709230	0.373900038559232	0.826371740591793	−3.26357267647820	−1.27016013830956
13	0.122329110997166	0.073922148708420	0.373900038555643	0.826371740585074	−3.26357267643772	−1.27016013829563
15	0.122329110997165	0.073922148708419	0.373900038555639	0.826371740585068	−3.26357267643768	−1.27016013829562
Varadan and Bhaskar (1991)	0.1223	0.0739	0.374	0.826	−3.264	−1.27

Table 6
Results of the convergence study for a symmetric three-ply cylindrical shell with $a/h=10$ under imposed transverse deformation.

I_n	$\bar{u}_3(0.5)$	$\bar{\sigma}_{11}(0.5)$	$\bar{\sigma}_{12}(0.5)$	$\bar{\sigma}_{13}(0)$	$\bar{\sigma}_{23}(0)$	$\bar{\sigma}_{33}(0)$
5	0.978593980499036	0.597511002024705	0.302185152960828	0.559672082814151	−26.3787979589690	−10.2629872834671
7	0.978567118243896	0.597371717350165	0.302151940656743	0.559749535705239	−26.3732391706573	−10.2642752706761
9	0.978567016077271	0.597371376040719	0.302151904703540	0.559749700202582	−26.7321744948760	−10.2642756271933
11	0.978567015861194	0.597371375516427	0.302151904726605	0.559749700568656	−26.3732174035435	−10.2642756223531
13	0.978567015860888	0.597371375515781	0.302151904726692	0.559749700569220	−26.3732174034771	−10.2642756223421
15	0.978567015860888	0.597371375515781	0.302151904726692	0.559749700569219	−26.3732174034771	−10.2642756223421

The data listed in Tables 5 and 6 show the results of the convergence study due to increasing the number of SaS for the moderately thick cylindrical shell with $R/h=10$ for both types of boundary conditions (45) and (46). A comparison with the exact solution (Varadan and Bhaskar, 1991) is also given. Figs. 4 and 5 display the through-thickness distributions of displacements and stresses for different values of the slenderness ratio R/h using nine SaS for each layer. These results demonstrate again the efficiency of the strong SaS formulation for the 3D stress analysis of layered composite shells.

6. Analytical solution for simply supported layered cylindrical panel

Consider a simply supported layered orthotropic cylindrical panel. The boundary conditions at the edges are expressed as

$$\begin{aligned} &\sigma_{11}^{(n)}=u_2^{(n)}=u_3^{(n)}=0 \quad \text{at } \theta_1=0 \text{ and } \theta_1=a,\\ &u_1^{(n)}=\sigma_{22}^{(n)}=u_3^{(n)}=0 \quad \text{at } \theta_2=0 \text{ and } \theta_2=b, \end{aligned} \tag{49}$$

where a is the length of the panel; $b=\varphi R$ is the length of the circular arc; φ is the arc angle. To satisfy boundary conditions (49), we search the analytical solution by a method of the double Fourier series expansion

$$\begin{aligned} u_1^{(n)i_n}&=\sum_{r=1}^{\infty}\sum_{s=1}^{\infty} u_{1rs}^{(n)i_n}\cos\tfrac{r\pi\theta_1}{a}\sin\tfrac{s\pi\theta_2}{b},\\ u_2^{(n)i_n}&=\sum_{r=1}^{\infty}\sum_{s=1}^{\infty} u_{2rs}^{(n)i_n}\sin\tfrac{r\pi\theta_1}{a}\cos\tfrac{s\pi\theta_2}{b},\\ u_3^{(n)i_n}&=\sum_{r=1}^{\infty}\sum_{s=1}^{\infty} u_{3rs}^{(n)i_n}\sin\tfrac{r\pi\theta_1}{a}\sin\tfrac{s\pi\theta_2}{b}, \end{aligned} \tag{50}$$

where r and s are the wave numbers in θ_1- and θ_2-directions. The surface loads are also expanded in double Fourier series.

Following the technique developed in Section 4, we substitute the Fourier series (50) in Eqs. (7), (8), (12), (24) and (26)–(32) that yields the systems of linear algebraic equations for finding the SaS displacement amplitudes of the nth layer $u_{irs}^{(n)i_n}$.

7. Conclusions

A strong SaS formulation based on direct integration of the equilibrium equations of elasticity for the 3D stress analysis of layered shells has been developed. The SaS are located at Chebyshev polynomial nodes throughout the layers. The use of only Chebyshev polynomial nodes allows one to minimize uniformly the error due to Lagrange interpolation. Therefore, the proposed strong SaS formulation makes it possible to derive the analytical solutions for simply supported layered cylindrical shells and cylindrical panels with a prescribed accuracy, which asymptotically approach the exact solutions of elasticity as the number of SaS goes to infinity.

The extension of the strong SaS formulation to functionally graded material (FGM) shells is straightforward following the variational SaS formulation (Kulikov and Plotnikova, 2014b, 2017). The implementation of the SaS method for layered FGM shells is based on the use of the same Lagrange interpolations for the material parameters through the thicknesses of layers. Owing to the Lagrange interpolation it does not matter what type of the material law is adopted in the SaS FGM shell formulation. In fact, the knowledge of only numerical values of the material properties on SaS is required.

Acknowledgments

This work was supported by the Russian Science Foundation (Grant No. 15-19-30002) and the Russian Ministry of Education and Science (Grant No. 9.4914.2017).

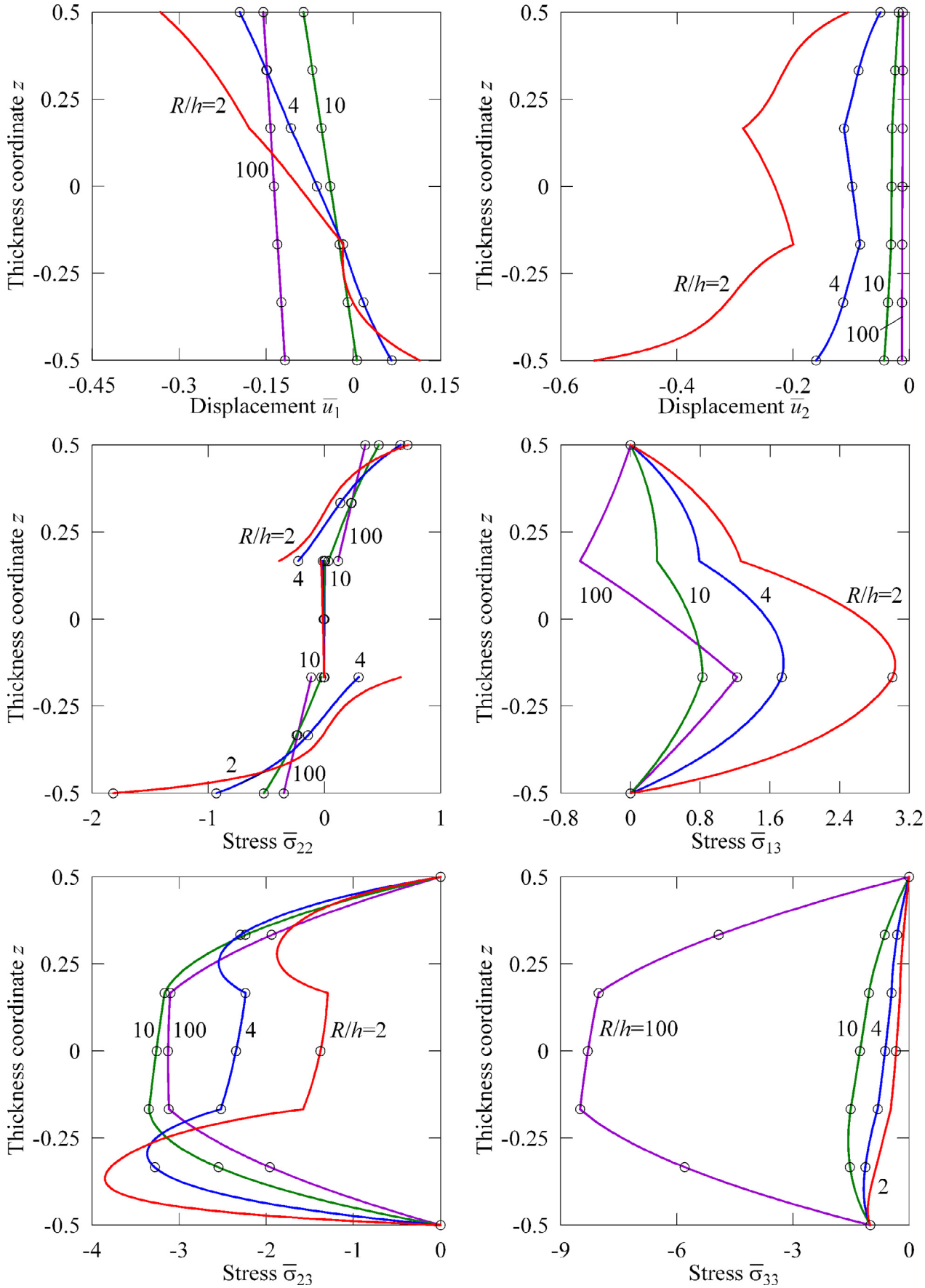

Fig. 4. Through-thickness distributions of displacements and stresses for a symmetric three-ply cylindrical shell under transverse loading for $I_1 = I_2 = I_3 = 9$: SaS formulation (——) and Varadan-Bhaskar exact solution (○).

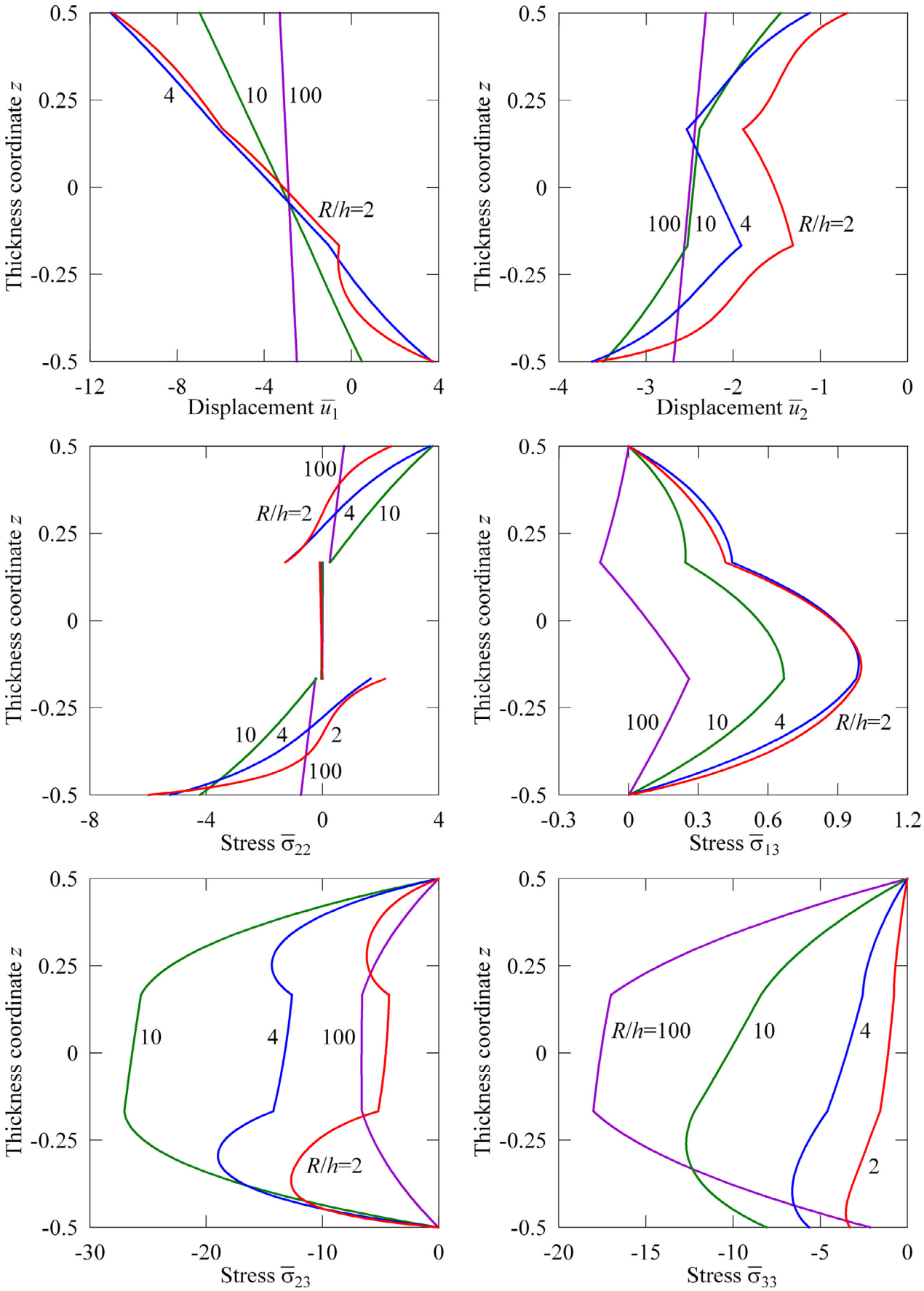

Fig. 5. Through-thickness distributions of displacements and stresses for a symmetric three-ply cylindrical shell under imposed transverse deformation for $I_1 = I_2 = I_3 = 9$.

References

Ambartsumyan, S.A., 1964. Theory of Anisotropic Shells. NASA TT F-118. NASA, Washington, D.C.

Bakhvalov, N.S., 1977. Numerical Methods: Analysis, Algebra, Ordinary Differential Equations. MIR Publishers, Moscow.

Brogan, W.L., 1985. Modern Control Theory. Prentice Hall, New Jersey.

Burton, W.S., Noor, A.K., 1994. Three-dimensional solutions for thermomechanical stresses in sandwich panels and shells. J. Eng. Mech. 120, 2044–2071.

Chen, C.Q., Shen, Y.P., 1996. Piezothermoelasticity analysis for a circular cylindrical shell under the state of axisymmetric deformation. Int. J. Eng. Sci. 34, 1585–1600.

Cheng, Z.Q., Reddy, J.N., 2002. Asymptotic theory for laminated piezoelectric circular cylindrical shells. AIAA J 40, 553–558.

Frobenius, G., 1873. Ueber die Integration der linearen Differentialgleichungen durch Reihen. J. Reine Angew. Math. 76, 214–235.

Gol'denveizer, A.N., 1961. Theory of Thin Elastic Shells. Pergamon Press, New York.

Heyliger, P., 1997. A note on the static behavior of simply-supported laminated piezoelectric cylinders. Int. J. Solids Struct. 34, 3781–3794.

Huang, N.N., Tauchert, T.R., 1991. Thermoelastic solution for cross-ply cylindrical panels. J. Thermal Stresses 14, 227–237.

Kapuria, S., Dumir, P.C., Sengupta, S., 1997a. Nonaxisymmetric exact piezothermoelastic solution for laminated cylindrical shell. AIAA J 35, 1792–1795.

Kapuria, S., Sengupta, S., Dumir, P.C., 1997b. Three-dimensional solution for simply–supported piezoelectric cylindrical shell for axisymmetric load. Comput. Methods Appl. Mech. Eng. 140, 139–155.

Kapuria, S., Sengupta, S., Dumir, P.C., 1997c. Three-dimensional solution for a hybrid cylindrical shell under axisymmetric thermoelectric load. Arch. Appl. Mech. 67, 320–330.

Kulikov, G.M., 2001. Refined global approximation theory of multilayered plates and shells. J. Eng. Mech. 127, 119–125.

Kulikov, G.M., Carrera, E., 2008. Finite deformation higher-order shell models and rigid-body motions. Int. J. Solids Struct. 45, 3153–3172.

Kulikov, G.M., Mamontov, A.A., Plotnikova, S.V., 2015. Coupled thermoelectroelastic stress analysis of piezoelectric shells. Compos. Struct. 124, 65–76.

Kulikov, G.M., Plotnikova, S.V., 2011. On the use of a new concept of sampling surfaces in a shell theory. Adv. Struct. Mater. 15, 715–726.

Kulikov, G.M., Plotnikova, S.V., 2012a. Exact 3D stress analysis of laminated composite plates by sampling surfaces method. Compos. Struct. 94, 3654–3663.

Kulikov, G.M., Plotnikova, S.V., 2012b. On the use of sampling surfaces method for solution of 3D elasticity problems for thick shells. ZAMM – J. Appl. Math. Mech. 92, 910–920.

Kulikov, G.M., Plotnikova, S.V., 2013a. Advanced formulation for laminated composite shells: 3D stress analysis and rigid-body motions. Compos. Struct. 95, 236–246.

Kulikov, G.M., Plotnikova, S.V., 2013b. A sampling surfaces method and its application to three-dimensional exact solutions for piezoelectric laminated shells. Int. J. Solids Struct. 50, 1930–1943.

Kulikov, G.M., Plotnikova, S.V., 2014a. Solution of three-dimensional problems for thick elastic shells by the method of reference surfaces. Mech. Solids 49, 403–412.

Kulikov, G.M., Plotnikova, S.V., 2014b. Exact electroelastic analysis of functionally graded piezoelectric shells. Int. J. Solids Struct. 51, 13–25.

Kulikov, G.M., Plotnikova, S.V., 2014c. 3D exact thermoelastic analysis of laminated composite shells via sampling surfaces method. Compos. Struct. 115, 120–130.

Kulikov, G.M., Plotnikova, S.V., 2016. Hybrid-mixed ANS finite elements for stress analysis of laminated composite structures: Sampling surfaces plate formulation. Comput. Methods Appl. Mech. Eng. 303, 374–399.

Kulikov, G.M., Plotnikova, S.V., 2017. Assessment of the sampling surfaces formulation for thermoelectroelastic analysis of layered and functionally graded piezoelectric shells. Mech. Adv. Mater. Struct. 24, 392–409.

Pagano, N.J., 1970. Exact solutions for rectangular bidirectional composites and sandwich plates. J. Compos. Mater. 4, 20–34.

Ren, J.G., 1989. Analysis of simply-supported laminated circular cylindrical shell roofs. Compos. Struct. 11, 277–292.

Shu, C., 2000. Differential Quadrature and Its Application in Engineering. Springer, Berlin.

Soldatos, K.P., Hadjigeorgiou, V.P., 1990. Three-dimensional solution of the free vibration problem of homogeneous isotropic cylindrical shells and panels. J. Sound. Vib. 137, 369–384.

Soldatos, K.P., Ye, J.Q., 1995. Stationary thermoelastic analysis of thick cross-ply laminated cylinders and cylindrical panels. Acta Mech 110, 1–18.

Srinivas, S., 1974. Analysis of laminated, composite, circular cylindrical shells with general boundary conditions. NASA TR R-412. NASA, Washington, D.C.

Tarn, J.Q., Yen, C.B., 1995. A three-dimensional asymptotic analysis of anisotropic inhomogeneous and laminated cylindrical shells. Acta Mech 113, 137–153.

Tornabene, F., Fantuzzi, N., Ubertini, F., Viola, E., 2015. Strong formulation finite element method based on differential quadrature: A survey. Appl. Mech. Rev. 67, 020801.

Varadan, T.K., Bhaskar, K., 1991. Bending of laminated orthotropic cylindrical shells–an elasticity approach. Compos. Struct. 17, 141–156.

Vel, S.S., 2011. Exact thermoelastic analysis of functionally graded anisotropic hollow cylinders with arbitrary material gradation. Mech. Adv. Mater. Struct. 18, 14–31.

Wang, X., Zhong, Z., 2003. A finitely long circular cylindrical shell of piezoelectric/piezomagnetic composite under pressuring and temperature change. Int. J. Eng. Sci. 41, 2429–2445.

Wu, C.P., Chiu, K.H., Wang, Y.M., 2008. A review on the three-dimensional analytical approaches of multilayered and functionally graded piezoelectric plates and shells. Comput. Mater. Continua 8, 93–132.

Wu, C.P., Liu, K.Y., 2007. A state space approach for the analysis of doubly curved functionally graded elastic and piezoelectric shells. Comput. Mater. Continua 6, 177–199.

Wu, C.P., Liu, Y.C., 2016. A review of semi-analytical numerical methods for laminated composite and multilayered functionally graded elastic/piezoelectric plates and shells. Compos. Struct. 147, 1–15.

Wu, C.P., Lo, J.Y., Chao, J.K., 2005. A three-dimensional asymptotic theory of laminated piezoelectric shells. Comput. Mater. Continua 2, 119–137.

Wu, C.P., Syu, Y.S., Lo, J.Y., 2007. Three-dimensional solutions for multilayered piezoelectric hollow cylinders by an asymptotic approach, Int. J. Mech. Sci. 49, 669–689.

Wu, C.P., Tsai, T.C., 2012. Exact solutions of functionally graded piezoelectric material sandwich cylinders by a modified Pagano method. Appl. Math. Model. 36, 1910–1930.

Xu, K., Noor, A.K., 1996. Three-dimensional analytical solutions for coupled thermo–electroelastic response of multilayered cylindrical shells. AIAA J 34, 802–810.

Ye, J.Q., Soldatos, K.P., 1994. Three-dimensional stress analysis of orthotropic and cross-ply laminated hollow cylinders and cylindrical panels. Comput. Methods Appl. Mech. Eng. 117, 331–351.